Available online at www.sciencedirect.com

ScienceDirect

Advances in Space Research 56 (2015) 1901–1910

ADVANCES IN SPACE RESEARCH (a COSPAR publication)

www.elsevier.com/locate/asr

Geographical analysis of equatorial plasma bubbles by GPS and nightglow measurements

D.P. Nade [a], D.J. Shetti [b], A.K. Sharma [c,*], A. Taori [d], G.A. Chavan [c], P.T. Patil [e], R.N. Ghodpage [e], O.B. Gurav [c], S.S. Nikte [f]

[a] *Department of Basic Sciences and Humanities, Sanjay Ghodawat Group of Institutions, Atigre, India*
[b] *Department of Physics, Smt. Kasturbai Walchand College, Sangli, India*
[c] *Earth and Space Science Laboratory, Department of Physics, Shivaji University, Kolhapur, India*
[d] *National Atmospheric Research Laboratory, Gadanki, India*
[e] *Medium Frequency Radar, Indian Institute of Geomagnetism, Shivaji University Campus, Kolhapur, India*
[f] *Department of Basic Sciences and Humanities, Vishveshwarya Technical Campus (VTC), Patgaon, Miraj, India*

Received 23 December 2014; received in revised form 20 March 2015; accepted 22 March 2015
Available online 27 March 2015

Abstract

This work about the zonal drift velocity and signature of equatorial plasma bubbles (EPBs) by measurements of global positioning system (GPS) receiver and all sky imager (ASI) operating in India, at the low latitude region. The optical and radio observations have been made from Kolhapur (16.8° N, 74.2° E) and Hyderabad (17.37°N, 78.48°E), respectively. The zonal drift velocity of EPBs has estimated using images of nightglow OI 630.0 nm emission recorded by ASI at Kolhapur. The measurements of total electron content (TEC) using the GPS have carried from the nearby station, Hyderabad. When depletions occurred about 00:37 h (IST) in TEC, the EPBs were found to occur about 5:30 h in optical data of OI 630.0 nm emission. This work focuses on simultaneous measurements of TEC and intensity of OI 630.0 nm emissions for EPBs during nighttime. The occurrence period of EPBs in TEC and OI 630.0 nm has found to be different. To study this difference, the zonal drift velocity of EPBs has established. The averaged eastward velocity of EPBs was found to be 138 m/s. The calculated values of zonal drift velocities are well correlated with that of the empirical model values. This work may be helpful in finding the growth of EPBs over low latitude.

Keywords: GPS; TEC; All sky imager; OI 630.0 nm emissions; Equatorial plasma bubbles

1. Introduction

In the F-region, at low latitude, plasma irregularities have been frequently observed due to the instability processes occurring in the ionized medium. Due to the depletions in electron density, as compared to the background density, the plasma irregularities are observed in optical data. These irregularities are also known as "equatorial plasma bubble" (EPB). At the dip equator, after sunset, plasma irregularities are generated in the bottom side of F- region mainly because of the Rayleigh–Taylor (R–T) instability (e.g., Kelley, 1989). In the evening sector, due to $E \times B$ drift, the plasma is lifted from magnetic equator and reaches higher altitudes (e.g., Kelley et al., 2011). This plasma diffuses downward along the magnetic field lines (Weber et al., 1978) to higher latitudes because of strong gravity force. Thus, two ionization crests are created on both the sides of the magnetic equator. This phenomenon is studied by Lin et al. (2007), Balan et al. (1997). The effect of strong gravity-waves and other instabilities on growth of EPBs has studied by Taori et al.

* Corresponding author.
E-mail address: aks_phy@unishivaji.ac.in (A.K. Sharma).

http://dx.doi.org/10.1016/j.asr.2015.03.030
0273-1177/

(2010) and Taori et al. (2011) respectively. These irregularities are making the scintillations in radio signals and thus error occurs in communication and navigation system.

The occurrence of EPBs have been studied using radar observations from Jicamarca, Peru (Chapagain et al., 2009), by scintillation technique (Chandra et al., 2003) and by ASI (e.g., Nade et al., 2012; Taori and Sindhya, 2013) in India and also from Cachoeira Paulista, Brazil (Sahai et al., 1994; Pimenta et al., 2001). The cosmic noise absorption measurement (at 30 MHz) has been done from Kolhapur to study the effect of solar noise and local noise on ionosphere (Nikte et al., 2014). Several investigators have been using ASI (OI 630.0 nm emission) to study the onset, evolution and dynamics of EPBs (e.g., Weber et al., 1980; Sahai et al., 1994; Taylor, 1997; Mukherjee and Shetti, 2008; Fagundes et al., 1999; Sinha et al., 2007; Taori et al., 2013). It is of scientific interest to study the characteristics and morphology of EPBs because they cause random error and scintillations in the satellite signals which results in barrier in communication and navigation system. Seker et al. (2007) identified the plasma depletion using coordinated VHF radar and airglow measurements from Gadanki. The plasma depletions are also called EPBs.

At F-region heights (250–300 km), at low latitude, the nightglow OI 630.0 nm emissions are generated (e.g., Pimenta et al., 2001). Terra et al. (2004) also reported that the peak emission altitude of OI 630.0 nm to be at heights around 250–280 km. This region is very important to study EPBs using OI 630.0 nm emissions. Dark patches in nightglow OI 630.0 nm images, due to low electrons density, are the signatures of EPBs. The F-region nightglow emission at (^{1}D) OI 630.0 nm, are governed by dissociative recombination between O_2^+ and electrons. The reaction mechanism is given below

$$O^+ + O_2 \rightarrow O_2^+ + O$$
$$O_2^+ + e \rightarrow O + O^*$$
$$O^* \rightarrow O + h\upsilon_{(630\ \text{nm})}$$

Here " * " sign on oxygen indicates the excited state; these excited atoms (oxygen) radiate 630.0 nm emissions.

This paper presents the zonal drift velocity and signature of EPBs in the measurements of TEC and intensity of OI 630.0 nm emission from the low latitude regions in India. Fig. 1 illustrates the location of ASI and GPS receiver at Kolhapur and Hyderabad respectively. Herein image of OI 630.0 nm shows the area covered by ASI from Kolhapur at an altitude 250 km. The red line indicates the dip equator (magnetic equator). The first section introduced the importance of ionospheric irregularities like EPBs and related studies. The second section discusses the experimental setup for TEC measurements and data of images of OI 630.0 nm. The results are presented in the third section and the fourth section gives new idea about results with respect to earlier studies in this field.

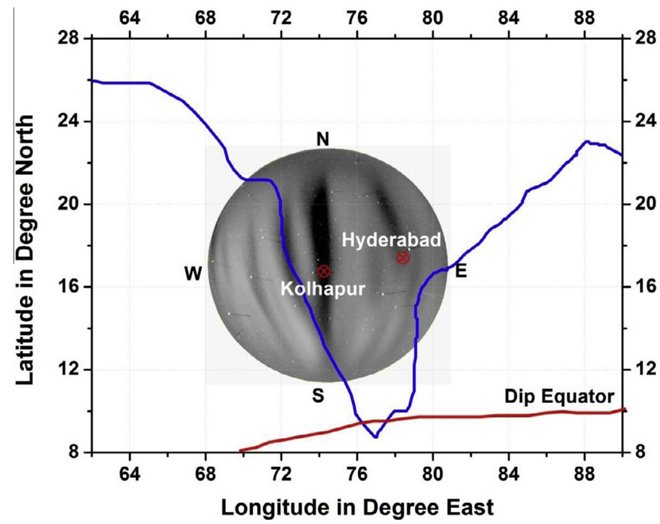

Fig. 1. The location of ASI and GPS receiver at Kolhapur and Hyderabad respectively. Nightglow OI 630.0 nm image shows the area covered by ASI from Kolhapur at an altitude 250 km. The red line indicates the dip equator (magnetic equator). (For interpretation of the references to color in this figure legend, the reader is referred to the web version of this article.)

2. Experimental setup

2.1. TEC measurements

Up to eleven GPS satellites are in view and provide outputs in 22 receiver channels (Dashora and Pandey, 2005). The ionosphere has an effect on the signal of GPS satellite. TEC is measured along the path from the GPS satellite to a receiver. The TEC is defined by the integral of electron density in TEC unit (TECU), where 1 TEC unit = 10^{16} electrons m^{-2} column along the signal transmission path. The dual frequency GPS receivers are used to measure the TEC, which is one of the most important methods to investigate the dynamics of ionosphere. Several research groups are showing interest in the equatorial ionospheric research using GPS data. Dow et al. (2009) did an analysis of the importance of GPS data in support of the terrestrial reference frame, earth observations and research, positioning, navigation and timing as well as other applications that benefit the society. The slant TEC is the measure of the total number of free electrons in a column of unit cross section along the path of the electromagnetic wave between the satellite and the receiver (Browne et al., 1956).

A dual frequency (L1 = 1575.42 MHz and L2 = 1227.60 MHz) GPS receiver (LEICA GRX1200GGPRO GNSS) is operating at Hyderabad (17.37° N, 78.48° E). It is a unique station to study the ionospheric irregularities because it is located at the northern crest of the equatorial ionization anomaly (EIA). A dual-frequency GPS receiver can measure the difference in ionospheric delays between the L1 and L2 of the GPS frequencies, which are generally assumed to travel along the same path through the ionosphere. Thus, the group delay can be obtained as

$$\Delta(\delta t) = \delta t_{L1} - \delta t_{L2}$$

Here, $\Delta(\delta t)$ is time delay in pseudo-range (δt_{L1}) at L1 and pseudo-range (δt_{L2}) at L2. The resulting equation is (Jain et al., 2011),

$$\Delta(\delta t) = 40.3 \times TEC \times \frac{(f_{L1}^2 - f_{L2}^2)}{(c \times f_{L1}^2 \times f_{L2}^2)}$$

where f_{L1} and f_{L2} are the group path lengths corresponding to the high and low GPS frequencies $f_{L1} = 1575.42$ and $f_{L2} = 1227.60$ MHz respectively and c is speed of light in vacuum. The TEC can be obtained by rewrite above equation as,

$$TEC = \frac{1}{40.3} \times \frac{(c \times f_{L1}^2 \times f_{L2}^2)}{(f_{L1}^2 - f_{L2}^2)} \times \Delta(\delta t)$$

The signal from different GPS satellites, at random elevation angles, recorded as a TEC measurements. These different satellites are identified by a pseudo-random number (PRN). The portions of the ionosphere cross by GPS signal depend on the elevation angle of GPS satellite. Therefore, in the present work the TEC data of only those GPS satellites, having elevation angles above 30° to avoid multipath effect of signals, are considered. The maximum elevation angle over Hyderabad station is 60°. The STEC is measured at every 30 s by the GPS receiver.

2.2. The nightglow OI 630.0 nm observations

The observations of nightglow OI 630.0 nm images are made from low latitude station Kolhapur (16.8°N, 74.2° and dip lat 10.6°N). It is located at the northern crest of the EIA and thus it is a unique location to study the F-region electrodynamics. Under scientific MoU between Shivaji University (SU), Kolhapur and Indian Institute of Geomagnetism (IIG), Navi Mumbai, a high resolution CCD (1024 × 1024 pixels) based with back-illuminated array of a pixel with 16 bits depth, ASI is operating at SU Campus, Kolhapur. The quantum efficiency of the ASI is >95%. ASI has low dark current (0.5 electrons/pixel/s) with low readout noise and high linearity. The fish eye lens (f/4 Mamiya RB67) having 24 mm focal length and tele-centric lens system are used to collect the signal coming through the atmosphere. There are six filter positions which can be used to study various emission lines originating at different ionospheric and thermospheric heights. The images in OI 630.0 nm, OI 557.7 nm, 840.0 nm, 846.0 nm, and OH Meinel bands at 720.0–910.0 nm and the transmission of background light in 857.0 nm are recorded with integration time of typically 120 s, 120 s, 06 s, 06 s, 90 s and 10 s, respectively. A more detailed discussion about this experimental setup is presented by Sharma et al. (2012) and Nade et al. (2013).

Sharma et al. (2014) presented the “averaging method” for image processing, flat fielding correction. This method involves, in first step, taking the average of an hour image-data and in second step, this averaged image was subtracted from each image of a same hour data. Due to this process, the signature of EPBs in images of OI 630.0 nm is clearly seen. All images have been processed by using this method. To study the nocturnal variation in intensity of OI 630 nm emission the average intensity of a square bin (5 × 5 pixel) of an individual image, corresponding to a circular field of view of ~1° along the zenith has taken. Herein, below 100 (arb. unit) intensity of nightglow OI 630.0 nm emission is considered the signature of EPBs.

3. Results

This work is presenting the observations of EPBs and its velocity variations on 3 nights of April 2011 by using intensity of OI 630.0 nm and TEC measurements, as a case study. These 3 nights communicated to be magnetically quiet. As an increase in geomagnetic activity may take many hours to influence drift velocities (Fejer et al., 2005). It might also be having an effect on intensity of OI 630.0 nm and TEC measurements. The magnetic and solar activities are the function of ΣKp index and F10.7 cm solar flux. So those nights having ΣKp greater than or equal to 26 as has magnetically “disturbed”. The ΣKp index and F10.7 cm were obtained from http://sec.noaa.gov. More detail about the observations of EPBs for these nights are given below.

The sudden reduction in TEC is known as depletion. When one or more EPBs occur across the line of sight of satellite, the depletions originate (Valladaras et al., 2004). DasGupta et al. (1983) reported general morphology of the TEC depletions and their association with strong VHF scintillations from the South American zone. For present work, simultaneous observations of TEC and nightglow OI 630.0 nm images have been taken to study the occurrence of EPBs over low latitude stations in India. The EPBs observed in TEC measurement from Hyderabad (location of GPS receiver) low latitude, station in India. Generally, the TEC is inversely correlated with elevation angle of GPS satellite. Thus the values of TEC decreases gradually with increase of satellite elevation angle (Dashora and Pandey, 2005). Therefore TEC data of only those GPS satellites, having elevation angle greater than 60°, is used for analysis.

The plasma density measured by TEC along the line-of-sight of satellite and receiver. Therefore a variation in TEC is nothing but the variation in the slant length or latitudinal variation in the plasma density. The data of intensity of OI 630.0 nm has taken into account to verify the depletions in TEC are the signature of EPBs. Weber et al. (1996) had shown strong correlation between TEC and airglow 630.0 nm depletions. However non-EPB-related processes could produce quick reductions in the TEC value, therefore it is difficult to identify TEC depletions (Bagiya et al., 2009).

3.1. Observation on 01–02 April 2011

Fig. 2 shows the variations in TEC obtained by GPS receiver from satellite (PRN-17) at Hyderabad station on 01–02 April 2011. The satellite covered whole night of 01–02 April 2011 and its average elevation angle was greater than 40° (maximum about 64° during the occurrence of EPBs). The depletions in TEC data is the signature of EPBs. The major depletions have been found in TEC at 22:26 IST and 22:46 IST (Indian Standard Time (IST) = Universal Time + 05:30:00 h). The EPBs are indicated by D_1 and D_2 respectively in Fig. 2. The period of occurrence of major EPBs in TEC found to be one hour on 01–02 April 2011. Values of ΣKp index (19) and solar flux F10.7 cm (109), suggested that the night of 01–02 April 2011 has been magnetically quite.

In addition to TEC measurements, the nightglow OI 630.0 nm images are taken into account for the same night. Fig. 3 illustrates the variations in the intensity of nightglow OI 630.0 nm emission on 01–02 April 2011. This intensity is calculated by above mentioned method. The intensity data is smoothed by averaging 10 points, which is indicated by red line. This line indicates the normal variation in the intensity. In Fig. 3, D_1 to D_6 shows the major EPBs occurred at 21:27 IST, 22:11 IST 23:53 IST 00:05 IST 01:41 IST and 02:00 IST in the intensity of OI 630.0 nm. The intensity of nightglow OI 630.0 nm emission shows the occurrence period of these EPBs to be 273 min (min) on 01–02 April 2011 while in TEC it shows only 20 min. Fig. 4 illustrates few processed images of OI 630.0 nm, taken on 01–02 April 2011, showing time evolution and structure of the EPBs. Fig. 4 shows the EPBs by D_1 and D_2 occurred during the period of ∼21:20 IST to ∼23:20 IST.

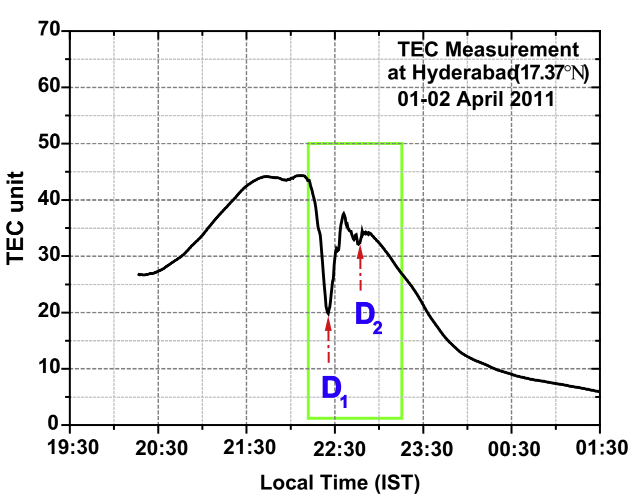

Fig. 2. The nocturnal variation in TEC with respect to local time (Indian Standard Time) observed on 01–02 April 2011. The EPBs in TEC is indicated by D_1 and D_2. The occurrence period of EPBs is indicated by rectangular.

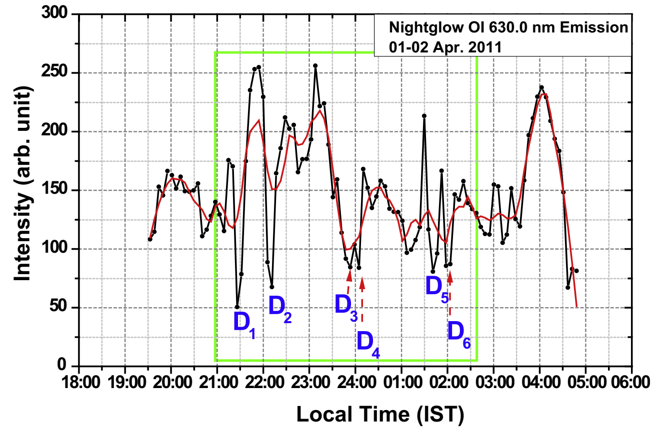

Fig. 3. The nocturnal variation in averaged intensity of OI 630.0 nm emissions is indicated by black line observed on 01–02 April 2011. The intensity data is smoothed by averaging 10 points indicates by red line. The EPBs are indicated by D_1 and D_6. The occurrence period of EPBs is indicated by rectangular. (For interpretation of the references to color in this figure legend, the reader is referred to the web version of this article.)

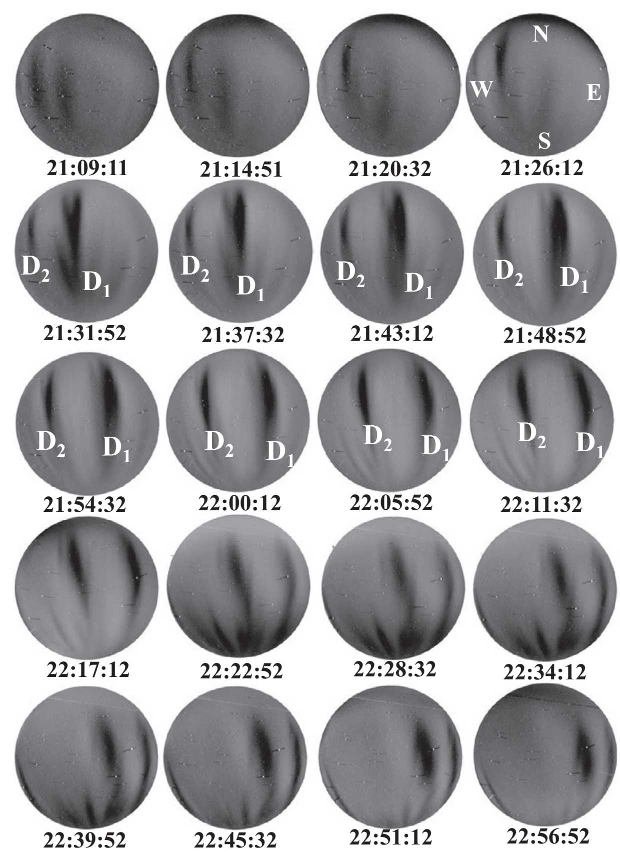

Fig. 4. The Sequence of images of OI 630.0 nm obtained on 01–02 April 2011 at different local time (LT).

3.2. Observation on 03–04 April 2011

Fig. 5 shows the variations in TEC measurements on 03–04 April 2011. The TEC data has obtained by GPS receiver from satellite (PRN-08). The elevation angle of

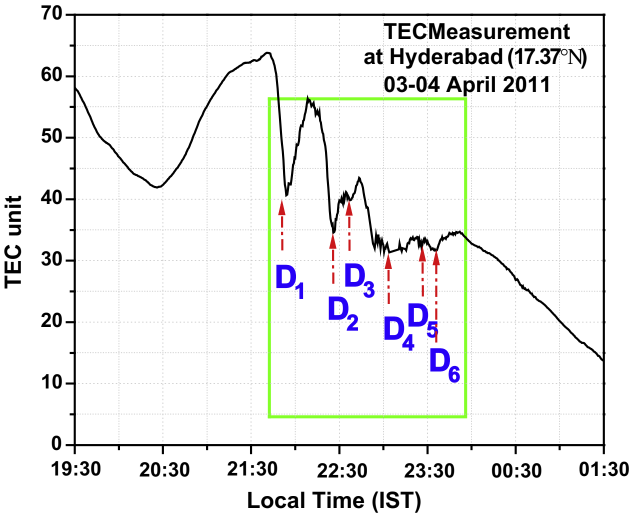

Fig. 5. The nocturnal variation in TEC with respect to local time observed on 03–04 April 2011. The EPBs in TEC is indicated by D_1 and D_6. The occurrence period of EPBs is indicates by rectangular.

PRN-08 had greater than 42° (averaged) and maximum about 75° during the occurrence of EPBs and also covered whole night of 03–04 April 2011. The signature of EPBs in TEC indicates by D_1 to D_6 in Fig. 4. These EPBs occurred at 21:55 IST, 22:26 IST, 22:39 IST, 23:00 IST, 23:25 IST, 23:25 IST and 23:36 IST respectively. The TEC measurement shows that occurrence period of EPBs was about 41 min on 03–04 April 2011. The values of ΣKp index and F10.7 cm were 25 and 114 respectively on 03–04 April 2011, indicating this night to be magnetically quite.

Fig. 6 illustrates the variations in intensity of OI 630.0 nm emissions obtained by cropped (5 × 5 pixel) images on 03–04 April 2011. In Fig. 5, the major EPBs indicate by D_1 to D_6. These six major EPBs had occurred at 21:16 IST, 21:33 IST, 22:35 IST, 00:00 IST, 02:17 IST and 03:14 IST on 03–04 April 2011 over Kolhapur. The nightglow OI 630.0 nm images are showing the occurrence period of EPBs about 360 min. The occurrence of EPBs in intensity of OI 630.0 nm and TEC data has verified by image data of OI 630.0 nm. Fig. 7 shows the sequence of some processed images of OI 630.0 nm obtained on 03–04 April 2011 from Kolhapur. The dark patches in images are the signature of EPBs. The north-west to south-east aligned EPBs moved towards the east.

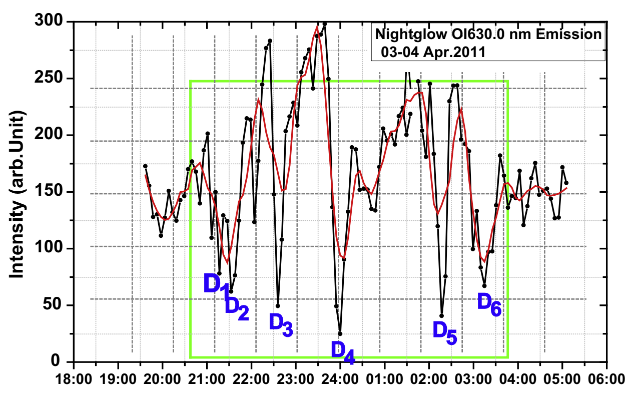

Fig. 6. The nocturnal variation in averaged intensity of OI 630.0 nm emissions is indicated by black line observed on 03–04 April 2011. The intensity data is smoothed by averaging 10 points indicates by red line. The EPBs are indicated by D_1 and D_6. The occurrence period of EPBs is indicated by rectangular. (For interpretation of the references to color in this figure legend, the reader is referred to the web version of this article.)

3.3. Observation on 05–06 April 2011

Fig. 8 illustrates the variations in TEC obtained by GPS receiver from satellite having PRN-08 on 05–06 April 2011. The elevation angle of PRN-08 had greater than 37° (averaged) and maximum about 64° during the occurrence of EPBs on 05–06 April 2011. In Fig. 8, the portion of occurrence of EPBs in TEC shows by rectangular (green color). The occurrence period of EPBs in TEC found to be about 171 min during 20:44 IST to 23:35 IST. Fig. 8 shows six major EPBs in TEC data occurred at 22:44 IST, 20:53 IST, 21:38 IST, 21:59 IST, 23:05 IST and 23:35 IST are indicating by D_1 to D_6 respectively in Fig. 8. The ΣKp index and F10.7 cm found to be 12 and 109 respectively

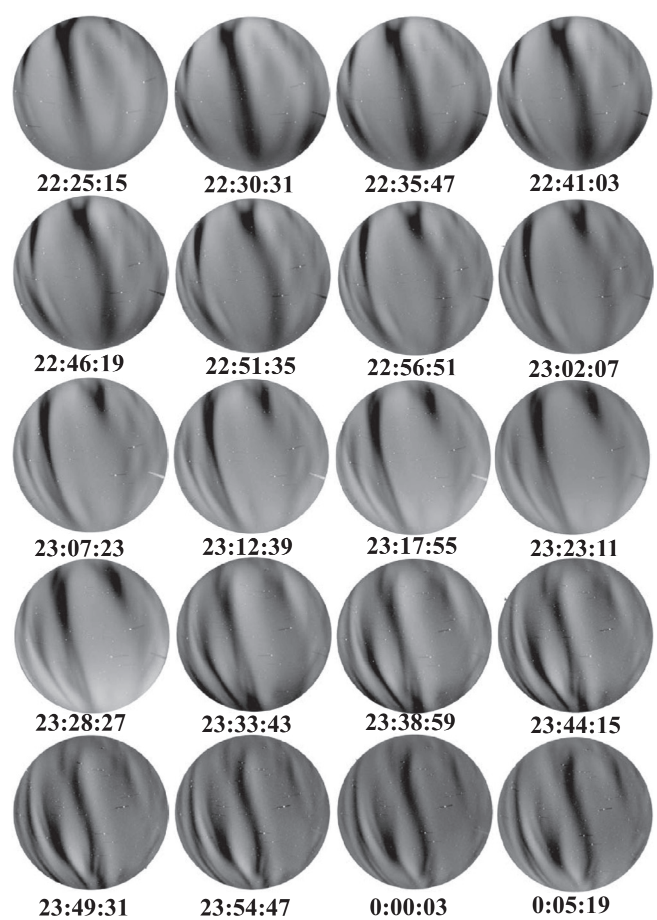

Fig. 7. The Sequence of images of OI 630.0 nm obtained on 03–04 April 2011 at different local time (LT).

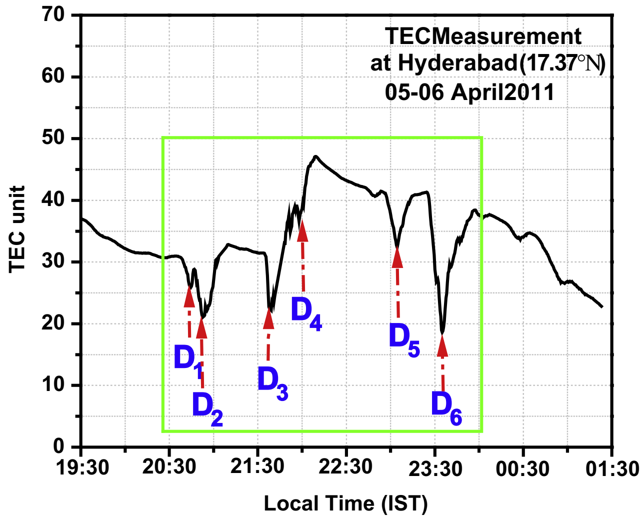

Fig. 8. The nocturnal variation in TEC with respect to local time on 05–06 April 2011. The EPBs in TEC is indicated by D_1 and D_6. The occurrence period of EPBs is indicates by rectangular.

on 05–06 April 2011. The night of 05–06 April 2011 had magnetically quite.

Fig. 9 illustrates the nocturnal variations in the intensity of nightglow OI 630.0 nm images, recorded on 05–06 April 2011. About five major EPBs has occurred over Kolhapur, these are indicating in intensity of OI 630.0 nm emissions at 20:51 IST, 22:16 IST, 22:30 IST, 23:38 IST and 01:17 IST on 05–06 April 2011. These EPBs shows by D_1 to D_5 respectively in Fig. 9. The images of OI 630.0 nm shows the occurrence period of EPBs found to be about 330 min from 20:51 IST to 01:17 IST on 05–06 April 2011. This period of occurrence is showing in Fig. 8 by rectangular (green color). Fig. 10 illustrates sequence of few processed images of OI 630.0 nm obtained on 05–06 April 2011.

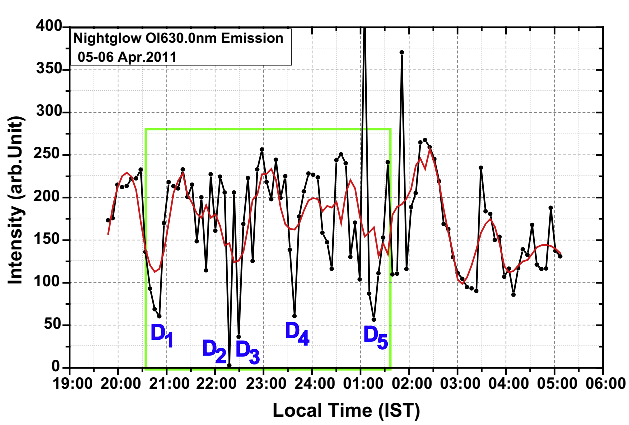

Fig. 9. The nocturnal variation in averaged intensity of OI 630.0 nm emissions is indicated by black line observed on 05–06 April 2011. The intensity data is smoothed by averaging 10 points indicates by red line. The EPBs are indicated by D_1 and D_5. The occurrence period of EPBs is indicated by rectangular. (For interpretation of the references to color in this figure legend, the reader is referred to the web version of this article.)

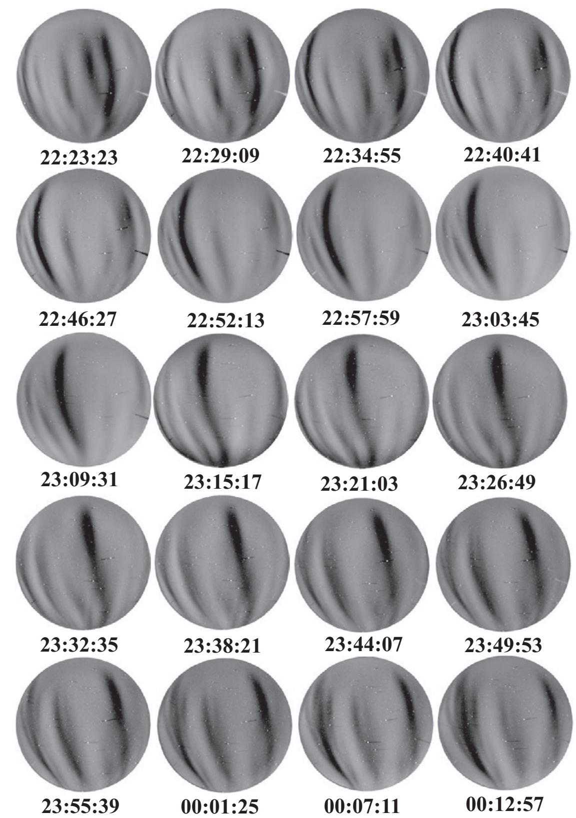

Fig. 10. Few sequences of images of OI 630.0 nm obtained on 05–06 April 2011 at different local time (LT).

3.4. Velocities of EPBs

The zonal drift velocity of EPBs calculated by comparing its positions in consecutive images to find the longitudinal offset and dividing it by the time difference between them (Makela and Kelley, 2003; Makela et al., 2005). Pimenta et al. (2001) proposed the "scanning method" to calculate drift velocity of EPB from OI 630.0 nm images. In this method, at first each image of OI 630.0 nm is scanned through the zenith (16.8°N) from east to west to obtain a cross-section of the depletion patterns for each EPB. These cross-sections are subjected to further analysis. The linearized images (Pimenta et al., 2001) with an appropriate geographic co-ordinate system (Garcia et al., 1997) had been used to compare the east–west intensity variations in consecutive images. A succession of EPBs in each image and their time shifts lead to a zonal velocity versus local time relation for EPB. The details of method have been described by Nade et al. (2013).

Steps involved in the calculation of zonal drift velocities of EPBs from OI 630.0 nm using scanning method is illustrating in Fig. 11. In Fig. 10, the upper panel (a) shows three images of OI 630.0 nm, taken on 03–04 April 2011 at 21:53:37 IST, 21:58:53 IST and 22:04:09 IST. The middle panel shows the east–west scan of depletion region obtained in these three images, lower panel indicates

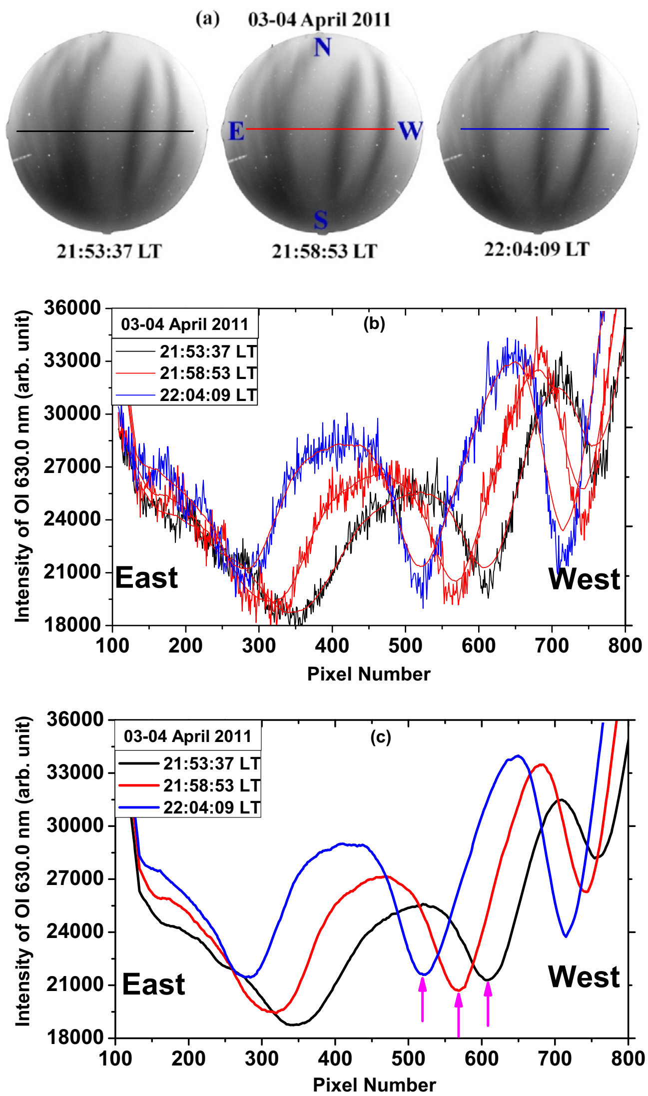

Fig. 11. The upper panel (a) shows images of OI 630.0 nm taken by ASI from Kolhapur at different time on 03–04 April 2011. The middle panel (b) shows east–west scan of EPBs showing in (a). The lower panel (c) shows east–west scanned data smoothed by 50 points averaged and pink arrows (in upward directions) indicates the center of EPBs (Nade et al., 2013). (For interpretation of the references to color in this figure legend, the reader is referred to the web version of this article.)

east–west scanned data smoothed by 50 points averaged and pink arrows (in upward directions) indicates the center of EPBs. The east–west scanned data has been smoothed by 50 points average to identify the boundaries of EPBs. In nightglow OI 630.0 nm intensity in arbitrary units (arb. unit) plot, the pink arrows (in upward directions) indicate the motion of center of EPB from the west to east. Due to unavailability of a standard source of light, the nightglow intensities have not been calibrated in Rayleigh, and hence, the intensities are presented in the arbitrary unit.

The pixel numbers are noted for center, western wall and eastern wall of each EPB. Then these pixel numbers had been converted into geographic values (km) by method described by Sharma et al. (2014). In this method, pixels of nightglow OI 630.0 nm image are converted into actual geographic values (km) by the following formula based on the geometry of airglow emission layer

$$\psi = \cos^{-1}\left(\frac{R_h^2 + R^2 - r^2}{2R_hR}\right) \tag{1}$$

$$Arc = Radius \times Angle = R_h \times \psi \tag{2}$$

where, ψ is earth centered angle, R is the mean radius of the earth, R_h is the sum of mean radius of the earth and height of airglow emission layer, and r is the distance between location of imager and signature of EPB in sky, obtained in OI 630.0 nm images. The special displacements of these EPBs have determined from successive images and then divided by time (time difference between these images). Thus velocity of EPBs obtained.

Only those images have taken, in their EPBs occurred at or near the zenith (in 100° FOV) center of image. The motion of western wall, center and eastern wall of EPB are determined using scanning method (Pimenta et al., 2001) with geometry method (Sharma et al., 2014). Fig. 12 shows the velocity of -western wall, center and eastern wall of EPBs, on 03–04 April 2011. Large variations are observed in their velocities as a function of time. Therefore average velocity of these three velocities is presented by red line along with standard deviation in Fig. 12. Herein average velocity is taken for more accuracy in further analysis.

Using these methods zonal drift velocity of EPBs have calculated for three nights. For more accuracy only average velocity of western wall velocity, eastern wall velocity and center velocity of EPBs have taken for presentation. The average zonal drift velocities of EPBs corresponding to nights of 01–02, 03–04 and 05–06 April 2011 shows in

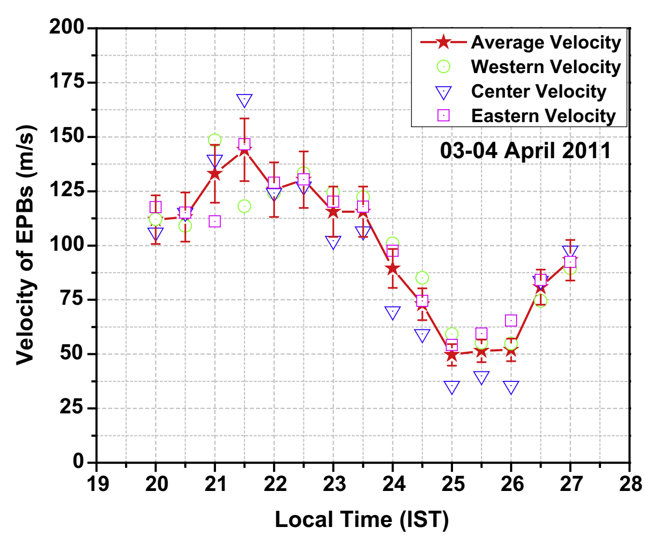

Fig. 12. The velocity of western wall, center and eastern wall of EPBs and average velocity of EPBs on 03–04 April 2011.

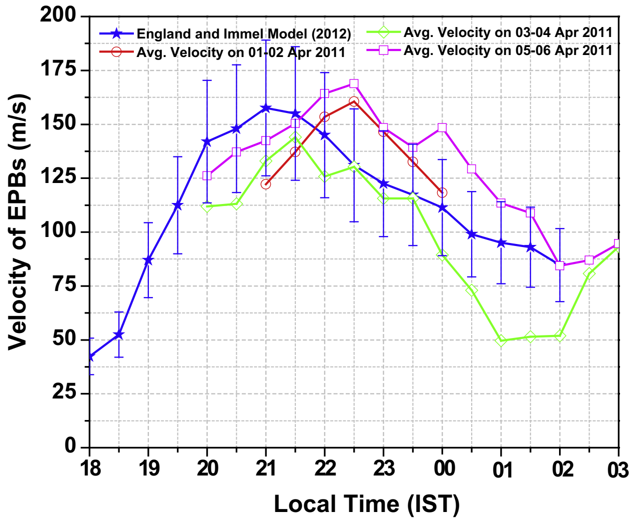

Fig. 13. The zonal drift velocity of EPBs as a function of local time (IST) compared with England and Immel model (2012).

Fig. 13. The calculated values of velocities using nightglow OI 630.0 nm images shows as red, green and pink lines for respectively nights. The empirical model values for zonal drift velocity of EPBs estimated by England and Immel, 2012 shows as solid blue line. The error bars in empirical model show the standard deviations representing the variability in the estimates. The calculated values have well matched with empirical model values.

From the evening, velocity increases till 21:30 to 22:30 IST and then it gradually decreases till the morning as function of local time. After sunset the ionospheric plasma instabilities increased (Fejer et al., 1999) due to dynamo of zonal (eastward) electric field in F-region. The intensity of electric field is very intense after sunset and decreases with time because of the reduced neutral wind velocity (Terra et al., 2004). de Paula et al. (2002) reported that the eastward zonal velocities of EPBs decrease after midnight. Results of present work has in good agreement with those of the previous studies in which the calculated average zonal velocity of EPB found to be ~140 m/s (Mukherjee et al., 1998). The maximum velocities have to be noted 160 m/s (at 22:30 IST), 144 m/s (at 21:30 IST), 168 m/s (at 22:30 IST) on 01–02, 03–04 and 05–06 April 2011 respectively.

4. Discussions

Table 1 shows the occurrence period of EPBs in TEC measurement and intensity of OI 630.0 nm emissions. According to Table 1, it is noted that occurrence probability of EPBs over Kolhapur has greater than Hyderabad. This might be due to the EPBs grouped over crests of the equatorial ionization anomaly. The geographical longitudinal differences between these two stations is ~1° latitude (=~111.2 km). It is observed that EPBs first occurred over Hyderabad and then over Kolhapur with maximum time period. These results suggest that EPBs have traveled towards the low latitude from magnetic equator.

The occurrence period of EPBs found in TEC measurements varied from night to night. Bagiya et al. (2009) also reported that the value of TEC varied from day to day, season and with solar activity. Thus, only these nights are selected for present work having magnetically quite. The zonal drift velocity of EPBs has calculated from images of OI 630.0 nm, to study the time variations in occurrence of EPBs over Hyderabad and Kolhapur.

The velocities of EPBs varied with latitude as well as altitude. Assumed an altitude difference in peak TEC and OI 630 nm emission has negligible. The latitudinal difference is very important to study the special displacement of EPBs in TEC and intensity of OI 630.0 nm. The eastward drift velocity of EPBs varies with time. The nighttime temporal variations in the zonal velocities of EPBs and plasma drift correlated well with the zonal neutral winds (Chapagain et al., 2013). The electric filed mapped along the entire magnetic field line. Thus plasma has built up in the flux tube and move with the neutral wind. The zonal drift velocity of EPBs was slower than that of the background neutral winds in evening time while after 23:00 LT they had nearly same in magnitude (Chapagain et al., 2012). Similar results found by Meriwether et al. (2013).

Thus difference in occurrence period is might be due to variations in velocity of EPBs. This result can be understood on the basis of the polarized electric field in F-region that drives the nocturnal variation in intensity of OI 630.0 nm emissions in that region. Bitten-court and Sahai (1978) reported the ionospheric plasma vertical drift produced by a horizontal thermospheric neutral wind at low latitudes. However, in the low latitude region, the electric field is generated by neutral winds (Haerendel and Eccles, 1992), which drives meridional Pedersen currents in the E

Table 1
Occurrence of EPBs in TEC measurements and intensity of nightglow OI 630.0 nm emissions over Hyderabad and Kolhapur.

Measurements	Date	01–02 April 2011		03–04 April 2011		05–06 April 2011	
	Time	IST	Minute	IST	Hours	IST	Minute
TEC at Hyderabad	Start Time	22:26	20	21:55	00:41	20:44	171
	End Time	22:46		22:36		23:35	
Intensity of OI 630.0 nm at Kolhapur	Start Time	21:27	273	21:16	05:58	20:51	326
	End Time	02:00		03:14		01:17	

and F regions. Therefore dynamo action has created in these regions.

5. Conclusions

Simultaneously, TEC measurements and nightglow OI 630.0 nm images has taken by GPS receiver at Hyderabad (17.37°N, 78.48°E) and ASI at Kolhapur respectively for the period of magnetically quite nights during April 2011.

The depletions in TEC have the signature of EPBs which has confirmed from nightglow intensity and images of OI 630.0 nm.

The averaged zonal drift velocities of EPBs well agree with the England and Immel (2012) model.

Time difference in occurrence of EPBs over Hyderabad and Kolhapur in TEC measurements and intensity nightglow of OI 630.0 nm respectively is might be due to variations in zonal drift velocity of EPBs. This may be the results of zonal polarized electric field and neutral wind.

The averaged zonal drift velocities of EPBs found eastward throughout night and reached maximum value of about 157 m/s around 20:30–21:30 IST and then decreased with time.

Acknowledgements

We are thankful to the NOAA-GOES team for providing the data of solar and geomagnetic indices on Internet. One of the authors Dr. D.P. Nade is also thankful to Mr. R.B. Mane (Sir) (J.B. Patil High School Chipari, Kolhapur) and Dr. R.P. Pawar for useful discussion on the generation of EPBs. One of the authors Dr. D.J. Shetti is also thankful to ISRO for providing funding through RESPOND programme.

References

Bagiya, M.S., Joshi, H.P., Iyer, K.N., Aggarwal, M., Ravindran, S., Pathan, B.M., 2009. TEC variations during low solar activity period (2005–2007) near the equatorial ionospheric anomaly crest region in India. Ann. Geophys. 27, 1047–1057.

Balan, N., Baile, G.J., Abdu, M.A., Oyama, K.I., Richards, P.G., MacDougall, J., Batista, I.S., 1997. Equatorial plasma fountain and its effects over three locations: evidence for an additional layer, the F3 layer. J. Geophys. Res. 102 (A2), 2047–2056.

Bitten-court, J.A., Sahai, Y., 1978. F-region neutral winds from ionosonde measurements of hmF2 at low-latitude magnetic conjugate regions. J. Atmos. Terr. Phys. 40, 669–676.

Browne, I.C., Evans, J.V., Hargreaves, J.V., Murray, J.A.W., 1956. Radio echoes from moon. Proc. Phys. Soc. (B) 69, 901–920.

Chandra, H., Sharma, S., Abdu, M.A., Batista, I.S., 2003. Spread-F at anomaly crest regions in the Indian and American longitudes. Adv. Space Res. 31, 717–727.

Chapagain, N.P., Fejer, B.G., Chau, J.L., 2009. Climatology of postsunset equatorial spread F over Jicamarca. J. Geophys. Res. 114, A07307. http://dx.doi.org/10.1029/2008JA013911.

Chapagain, N.P., Makela, J.J., Meriwether, J.W., Fisher, D.J., Buriti, R.A., Medeiros, A.F., 2012. Comparison of nighttime zonal neutral winds and equatorial plasma bubble drift velocities over Brazil. J. Geophys. Res. 117, A06309. http://dx.doi.org/10.1029/2012JA017620.

Chapagain, N.P., Fisher, D.J., Meriwether, J.W., Chau, J.L., Makela, J.J., 2013. Comparison of zonal neutral winds with equatorial plasma bubble and plasma drift velocities. J. Geophys. Res. 118, 1802–1812. http://dx.doi.org/10.1002/jgra.50238.

DasGupta, A., Basu, S., Aarons, J., Klobuchar, J.A., Bushby, A., 1983. VHF amplitude scintillation and associated electron content depletions as observed at Arequipa, Peru. J. Atmos. Terr. Phys. 45, 15–19.

Dashora, N., Pandey, R., 2005. Observations in equatorial anomaly region of total electron content enhancements and depletions. Ann. Geophys. 23, 2449–2456.

de Paula, E.R., Kantor, I.J., Sobral, J.H.A., Takahashi, H., Santana, D.C., Gobbi, D., Medeiros, A.F., Limiro, L.A.T., Kil, H., Kintner, P.M., Taylor, M.J., 2002. Ionospheric irregularity zonal velocities over Cachoeira Paulista. J. Atmos. Terr. Phys. 64, 1511–1516.

Dow, J.M., Neilan, R.E., Rizos, C., 2009. The International GNSS Service in a changing landscape of Global Navigation Satellite Systems. J. Geodesy 83 (3–4), 191–198.

England, S.L., Immel, T.J., 2012. An empirical model of the drift velocity of equatorial plasma depletions. J. Geophys. Res. 117, A12308. http://dx.doi.org/10.1029/2012JA018091,2012.

Fagundes, P.R., Sahai, Y., Batista, I.S., Abdu, M.A., Bittencourt, J.A., Takahashi, H., 1999. Observations of day-to-day variability in precursor signatures to equatorial F-region plasma depletions. Ann. Geophys. 17, 1053–1063.

Fejer, B.G., Scherliess, L., de Paula, E.R., 1999. Effects of the vertical plasma drift velocity on the generation and evolution of equatorial spread F. J. Geophys. Res. 104, 19859–19870.

Fejer, B.G., de Souza, J., Santos, A.S., Costa, P.A.E., 2005. Climatology of F-region zonal plasma drifts over Jicamarca. J. Geophys. Res. 110, A12310. http://dx.doi.org/10.1029/2005JA011324.

Garcia, F.J., Taylor, M.J., Kelley, M.C., 1997. Two-dimensional spectral analysis of mesospheric airglow image data. Appl. Opt. 36 (29), 7374–7385.

Haerendel, G., Eccles, J.V., 1992. The role of the equatorial electrojet in the evening ionosphere. J. Geophys. Res. 97, 1181–1192.

Jain, A., Tiwari, S., Jain, S., Gwal, A.K., 2011. Nighttime enhancements in TEC near the crest of northern equatorial ionization anomaly during low solar activity period. Indian J. Phys. 85 (9), 1367–1380.

Kelley, M.C., 1989. The Earth's Ionosphere, Int. Geophys. Ser., vol. 43, Academic, San Diego, Calif.

Kelley, M.C., Makela, J.J., de La Beaujardière, O., Retterer, J., 2011. Convective ionospheric storms: a review. Rev. Geophys. 49, RG2003. http://dx.doi.org/10.1029/2010RG000340.

Lin, C.H., Liu, J.Y., Fang, T.W., Chang, P.Y., Tsai, H.F., Chen, C.H., Hsiao, C.C., 2007. Motions of the equatorial ionization anomaly crests imaged by FORMOSAT-3/COSMIC. Geophys. Res. Lett. 34, L19101. http://dx.doi.org/10.1029/2007GL030741.

Makela, J.J., Kelley, M.C., 2003. Field-aligned 777.4-nm composite airglow images of equatorial plasma depletions. Geophys. Res. Lett. 30 (8), 1442. http://dx.doi.org/10.1029/2003GL017106.

Makela, J.J., Kelley, M.C., Su, S.-Y., 2005. Simultaneous observations of convective ionospheric storms: ROCSAT-1 and ground-based imagers. Space Weather 3, S12C02. http://dx.doi.org/10.1029/2005SW000164.

Meriwether, J.W., Makela, J.J., Fisher, D.J., Buriti, R.A., Medeiros, A.F., Akmaev, R.A., Fuller-Rowell, T.J., Wu, F., 2013. Comparisons of thermospheric wind and temperature measurements in equatorial Brazil to whole atmosphere model predictions. J. Atmos. Terr. Phys. 103, 103–112.

Mukherjee, G.K., Shetti, D.J., 2008. Plasma drift motion in F-region of ionosphere using photometric nightglow measurements. Indian J. Radio Space Phys. 37, 249–257.

Mukherjee, G.K., Carlo, L., Mahajan, S.H., Patil, P.T., 1998. First results of all-sky imaging from India. Earth Planets Space 50, 119–127.

Nade, D.P., Sharma, A.K., Nikte, S.S., Ghodpage, R.N., Patil, P.T., Rokade, M.V. Vhatkar, R.S., 2012. Occurrence of F-region plasma bubble over low latitude station: Kolhapur. In: Proceedings of

CARCAN-2012, Hyderabad, 21–22 Dec 2012, pp. 94–99. (ISBN: 978-93-82570-04-2).

Nade, D.P., Sharma, A.K., Nikte, S.S., Patil, P.T., Ghodpage, R.N., Rokade, M.V., Gurubaran, S., Taori, A., Sahai, Y., 2013. Zonal velocity of the equatorial plasma bubbles over Kolhapur, India. Ann. Geophys. 31, 2077–2084.

Nikte, S.S., Sharma, A.K., Rokade, M.V., Nade, D.P., Ghodpage, R.N., Patil, P.T., Bhonsle, R.V., 2014. Difficulties in the study of cosmic radio noise absorption at 30 MHz using riometer at low latitude station, Kolhapur (Lat-16.8°N, Long-74.25°E). Adv. Space Res. 53, 237–242.

Pimenta, A.A., Fagundes, P.R., Bittencourt, J.A., Sahai, Y., Gobbi, D., Medeiros, A.F., Taylor, M.J., Takahashi, H., 2001. Ionospheric plasma bubble zonal drift: a methodology using OI 630 nm all-sky imaging systems. Adv. Space Res. 27, 1219–1224.

Sahai, Y., Aarons, J., Mendillo, M., Baumgardner, J., Bittencourt, J.A., Takahashi, H., 1994. OI 630 nm imaging observations of equatorial plasma depletions at 16° S dip latitude. J. Atmos. Terr. Phys. 56, 1461–1475.

Seker, I., Mathews, J.D., Wiig, J., Gutierrez, P.F., Friedman, J.S., Tepley, C.A., 2007. First results from the Penn state all sky imager at Arecibo observatory. Earth Planets Space 59, 165–176.

Sharma, A.K., Nade, D.P., Nikte, S.S., Ghodpage, R.N., Patil, P.T., Rokade, M.V., Vhatkar, R.S., 2012. Analysis of plasma bubbles observed in night airglow emission line OI 630.0 nm from Kolhapur using all sky imager. Int. J. Eng. Sci. Res. 3 (2), 746–750.

Sharma, A.K., Nade, D.P., Nikte, S.S., Ghodpage, R.N., Patil, P.T., Rokade, M.V., Vhatkar, R.S., Gurubaran, S., 2014a. Development of fast image analysis technique for all sky images. Curr. Sci. 106 (8), 1085–1093.

Sharma, A.K., Nade, D.P., Nikte, S.S., Ghodpage, R.N., Patil, P.T., Rokade, M.V., Vhatkar, R.S., Gurubaran, S., 2014b. Occurrence of equatorial plasma bubbles over Kolhapur. Adv. Space Res. 54 (3), 435–442.

Sinha, H.S.S., Rajesh, P.K., Misra, R.N., Dutt, N., 2007. Multi-wavelength imaging observations of plasma depletions over Kavalur, India. Ann. Geophys. 19, 1119–1131.

Taori, A., Sindhya, A., 2013. Measurements of equatorial plasma depletion velocity using 630 nm airglow imaging over a low-latitude Indian station. J. Geophys. Res. Space Phys. 118. http://dx.doi.org/10.1002/2013JA019465.

Taori, A., Makela, J.J., Taylor, M., 2010. Mesospheric wave signatures and equatorial plasma bubbles: a case study. J. Geophys. Res. 115 (46), A06302. http://dx.doi.org/10.1029/2009JA015088.

Taori, A., Patra, A.K., Joshi, L.M., 2011. Gravity wave seeding of equatorial plasma bubbles: an investigation with simultaneous F-region, E-region and middle atmospheric measurements. J. Geophys. Res. 116. http://dx.doi.org/10.1029/2010JA016229.

Taori, A., Jayaraman, A., Kamalakar, V., 2013. Imaging of mesosphere–thermosphere airglow emissions over Gadanki (13.5°N, 79.2°E) first results. J. Atmos. Terr. Phys. 93, 21–28.

Taylor, M.J., 1997. A review of advances in imaging techniques for measuring short period gravity waves in the mesosphere and lower thermosphere. Adv. Space Res. 19 (4), 667–676.

Terra, P.M., Sobral, J.H.A., Abdu, M.A., Souza, J.R., Takahashi, H., 2004. Plasma bubble zonal velocity variations with solar activity in the Brazilian region. Ann. Geophys. 22, 3123–3128.

Valladaras, C.E., Villalobos, J., Sheehan, R., Hagan, M.P., 2004. Latitudinal extension of low-latitude scintillations measured with a network of GPS receivers. Ann. Geophys. 22, 3155–3175.

Weber, E.J., Buchau, J., Eather, R.H., Mende, S.B., 1978. North–south aligned equatorial airglow depletions. J. Geophys. Res. 83, 712–716.

Weber, E.J., Buchau, J., Moore, J.G., 1980. Airborne studies of equatorial F-layer ionospheric irregularities. J. Geophys. Res. 85, 4631–4641.

Weber, E.J., Basu, S., Bullet, T.W., Valladares, C.E., Bishop, G., Groves, K., Kuenzler, H., Ning, P., Sultan, P.J., Sheehan, R.E., Araya, J., 1996. Equatorial plasma depletion precursor signatures and onset observed at 11° south of the magnetic equator. J. Geophys. Res. 101, 26,829–26,838.